



Antimicrobial activity of novel cobalt(II) complexes with Schiff base derived from L-cysteine and 2-substituted benzaldehyde

Mirha Pazalja^{1*}, Irma Mahmutović-Dizdarević², Sabina Begić³, Alisa Smajović¹, Anesa Jerković-Mujkić², Monia Avdić^{4,5} and Mirsada Salihović¹

¹University of Sarajevo-Faculty of Pharmacy, Zmaja od Bosne 8, 71000 Sarajevo, Bosnia and Herzegovina.

²University of Sarajevo-Faculty of Science, Department of Biology, Zmaja od Bosne 33-35, 71000 Sarajevo, Bosnia and Herzegovina.

³University of Sarajevo-Faculty of Science, Department of Chemistry, Zmaja od Bosne 33-35, 71000 Sarajevo, Bosnia and Herzegovina.

⁴International Burch University, Department of Genetics and Bioengineering, Francuske revolucije bb, 71210 Iliđa, Bosnia and Herzegovina.

⁵Academy of Sciences and Arts of Bosnia and Herzegovina, Center for Disease Control and Geohealth Studies, Bistrik 7, 71000 Sarajevo, Bosnia and Herzegovina.
Email: mirha.pazalja@ffsa.unsa.ba

Received 17 November 2022; Received in revised form 28 April 2023; Accepted 7 July 2023

ABSTRACT

Aims: The aim of this study was to conduct antimicrobial analysis on novel Schiff base-derived cobalt(II) complexes (Co(L1)₂ and Co(L2)₂).

Methodology and results: Synthesis of Co(II) Schiff base complexes was carried out by reacting Schiff bases with cobalt(II) chloride hexahydrate and spectroscopic analyses were used for characterization. Microbiological assays comprised the determination of the minimum inhibitory concentration (MIC) and minimum bactericidal concentration (MBC) of tested substances and the evaluation of their antibiofilm activity. A total of 11 bacteria were tested, including multidrug-resistant strains. Investigated compounds performed inhibitory activity against all tested bacteria, with the MIC value of 250 µg/mL and 125 µg/mL just for *Escherichia coli* ATCC 14169. Results regarding the antibiofilm properties suggest that investigated Schiff's base complexes have antibiofilm activity in a strain-specific and concentration-dependant manner.

Conclusion, significance and impact of study: The current study showed that the novel complex compounds possess antimicrobial and antibiofilm properties against Gram-positive and Gram-negative bacteria. Since bacterial resistance to currently available antibiotics is rapidly increasing, further studies may provide information about using novel complexes as potential antimicrobial agents.

Keywords: Antibiofilm activity, cobalt(II) complex, minimum inhibitory concentration, minimum bactericidal concentration

INTRODUCTION

During the last few decades, great attention has been focused on studies of the Schiff bases for their pharmacological properties, such as antifungal, antibacterial and antitumor activity (Salihović *et al.*, 2018; Abu-Yamin *et al.*, 2022). Furthermore, Schiff bases play an important role in chemistry as ligands (Tsantis *et al.*, 2020). Schiff bases, which are derived from the condensation reaction of amino acids and aldehyde, are considered an important class of ligands that coordinate with metal ions *via* nitrogen from the azomethine group, phenolic oxygen and deprotonated carboxylate oxygen (Abu-Dief and Mohamed, 2015). Other atoms with free

electron pairs, such as sulfhydryl sulfur, can also form coordination bonds. Schiff base ligands are simple to synthesize and can form complexes with nearly any metal ion. Because their activity is generally increased by complexation with various metal ions, understanding the properties of ligands and metals can lead to the synthesis of highly active compounds. The results for antimicrobial activity showed that the metal complexes have significantly better antimicrobial activity than the ligand (Schiff base). By complexing, Schiff's base becomes a more powerful and potent antibacterial agent (Hossain *et al.*, 2018). Many Schiff bases complexes with cobalt have also attracted attention due to their broad range of biological and pharmaceutical activities, including

antioxidative, antitumor and antiviral properties (Ambika *et al.*, 2019; Bajema *et al.*, 2019; Shah *et al.*, 2020; Kar *et al.*, 2022). Moreover, many research groups have reported the catalytic activity of cobalt complexes (Gupta and Sutar, 2008; Banerjee and Chattopadhyay, 2019; Skrodzki *et al.*, 2021).

Salihović *et al.* (2021) recently published a paper describing the synthesis, characterization and antimicrobial activity of some Schiff bases derived from *L*-cysteine and aldehydes. Literature data showed that most Co(II) complex compounds have better antimicrobial activity than the Schiff bases that were used as ligands (Nejo *et al.*, 2010; Rajee *et al.*, 2021; Siraj and Sanusi, 2021). Due to those above, we used the previously prepared Schiff base to synthesize new Co(II) complexes. The synthesis, spectral characterization, and antimicrobial activity of new Co(II) complexes of *L*-cysteine and benzaldehyde-derived Schiff bases are described in this manuscript.

MATERIALS AND METHODS

Materials and instruments

All the chemicals used were analytical reagent grade and used without further purification. *L*-cysteine was from Sigma-Aldrich (St Louis, MO, USA), while 2-chlorobenzaldehyde and 2-methoxybenzaldehyde were from Merck (Darmstadt, Germany). Cobalt(II) chloride hexahydrate (CoCl₂·6H₂O) was purchased from Sigma-Aldrich (St Louis, MO, USA). A Koffler apparatus was used to determine the melting point. The infrared spectra of the synthesized compounds were obtained on potassium bromide pastilles with a Perkin Elmer Spectrum BX FTIR System in the range 400-4000/cm. To record UV spectra, the substances were dissolved in dimethyl sulfoxide (DMSO, Sigma-Aldrich, USA). The concentrations of the prepared solutions were 10⁻⁴ mol dm⁻³. The absorbance was measured on a spectrophotometer (UV-1280, Shimadzu) from 250 to 700 nm. TLC (thin layer chromatography) on Silica-TLC Alu foils (Fluka, Germany) plates were used to monitor the purity of the synthesized compounds and spots were visualized using a UV lamp (UVP 95-0072-09 Model C-10E4).

Procedure for preparation of Co(II) complexes Co(L1)₂ and Co(L2)₂

Schiff bases [2-((2-chlorobenzylidene) amino)-3-mercaptopropanoic acid] (L1) and 3-mercapto-2-[(2-methoxybenzylidene) amino] propanoic acid (L2), were prepared according to the literature procedure (Salihović *et al.*, 2021). The solution of Schiff bases (1 mmol: 243.01 mg L1, 239.39 mg L2) in 20 cm³ methanol was stirred for about 30 min at 40 °C. The Co(II) complexes with Schiff bases as ligands were synthesized according to a modified literature procedure (Nair *et al.*, 2012). The 10 cm³ solution of CoCl₂·6H₂O (0.50 mmol, 118.95 mg) was added dropwise to solutions of appropriate Schiff bases.

The reaction mixture was refluxed for 3 h with constant stirring at 65 °C. After the accomplishment of the reaction, which TLC monitored, the resulting solutions were evaporated on a rotavapor at 50 °C. Afterwards, reducing the volume of the solution, the residues were cooled to 0 °C (12 h) and then filtered, recrystallized and dried in a desiccator. Recrystallization from methanol produced brown Co(L1)₂ and emerald green Co(L2)₂ compounds, with 62% and 79% yields, respectively.

L1: m. p.: 179 °C, IR (KBr) ν (cm⁻¹): 3466 (OH), 1711 (C=O), 504 (Cl), 2932 (SH), 1611 (C=N), 2932 (C-H), 1441 (C=C). UV-Vis bands (nm): $\pi \rightarrow \pi^*$, 265, 275; $n \rightarrow \pi^*$, 432, 464.

Co(L1)₂ complex: m. p.: 270 °C, IR (KBr) ν (cm⁻¹): 1602 (C=N), 1400 (C-O(H)), 2928 (SH), 513 (Co-N), 435 (Co-O). UV-Vis bands (nm): $\pi \rightarrow \pi^*$, 261.50, 293; $n \rightarrow \pi^*$, 431, 443; *d-d*, 662.50.

L2: m.p.: 141 °C, IR (KBr) ν (cm⁻¹): 3436 (OH), 1739 (C=O), 1247 (O-CH₃), 2838 (SH), 1639 (C=N), 3053 (C-H), 1436 (C=C). UV-Vis bands (nm): $\pi \rightarrow \pi^*$, 255, 278.50; $n \rightarrow \pi^*$, 390, 429.

Co(L2)₂ complex: m.p.: 298 °C, IR (KBr) ν (cm⁻¹): 1631 (C=N), 1385 (C-O(H)), 2842 (SH), 534 (Co-N), 423 (Co-O). UV-Vis bands (nm): $\pi \rightarrow \pi^*$, 280.50, 315.50; $n \rightarrow \pi^*$, 408, 432.50, *d-d*, 673.50.

Antimicrobial activity

Bacterial strains

Tested Gram-positive bacteria included: *Staphylococcus aureus* subsp. *aureus* Rosenbach ATCC 6538 (SA1); *S. aureus* subsp. *aureus* Rosenbach ATCC 25923 (SA2); *S. aureus* subsp. *aureus* Rosenbach ATCC 33591, MRSA (SA3); *S. aureus* NCTC 12493, MRSA (SA4); *Enterococcus faecalis* ATCC 29212 (EF); and *Bacillus subtilis* subsp. *spizizenii* ATCC 6633 (BS). Gram-negative bacteria examined in the study were: *Escherichia coli* (Migula) Castellani and Chalmers ATCC 14169 (EC1); *E. coli* (Migula) Castellani and Chalmers ATCC 25922 (EC2); *E. coli* (Migula) Castellani and Chalmers ATCC 35218, ESBL (extended-spectrum β -lactamase producing) strain (EC3); *Salmonella enterica* subsp. *enterica* serotype Abony NCTC 6017 (SE); and *Pseudomonas aeruginosa* ATCC 27853 (PA). Bacterial inoculums were prepared, from overnight cultures, in a sterile saline solution to final turbidity of 0.50 McFarland standard corresponding to a microbial cell concentration of 1.50 × 10⁸ CFU/mL.

Broth microdilution method

The minimum inhibitory concentration (MIC) of Co(L1)₂ and Co(L2)₂ was determined using the broth microdilution method (CLSI, 2018). Both of the tested substances were dissolved in DMSO to a final concentration of 1 mg mL⁻¹. In 96-well plates, two-fold dilutions, in a final volume of 100 μ L of the same, were prepared in Mueller Hinton broth (Sigma-Aldrich, USA) in a total of 10 decreasing

concentrations. A 10 μL inoculum of the tested bacterial strain was added to each of the tested wells. Uninoculated media with the solvent were used as the negative control, while the positive control was the pure culture of each tested bacterial strain. The results were read after overnight incubation using the microplate reader (Biochrom EZ Read 400) at a wavelength of 595 nm. All experiments were performed in quadruplets. Minimum bactericidal concentration (MBC) was evaluated by replating the bacteria on sterile Mueller Hinton agar and determining the presence of growth after overnight incubation.

Tissue culture plate method

Biofilm formation in the presence of the tested substances was determined by using the Tissue Culture Plate method (TCP) in 96-well plates (Merritt *et al.*, 2005), where the diluting medium was Tryptic Soy Broth, TSB (Sigma-Aldrich, USA). An initial concentration of the tested substance of 1 mg/mL was diluted two-fold in TSB to an end concentration of 1.95×10^{-3} mg/mL with a final volume of 100 μL per well. Each of the wells containing the tested substance was inoculated with 10 μL of the tested bacterial culture (turbidity of 0.50 McFarland standard) prepared as described above. Uninoculated media with solvent was used as a negative control, while the biofilm formation of the tested strains was determined by evaluating their adherence only in the presence of TSB. After overnight incubation, the content of the plates was decanted, and the plates were washed in phosphate buffered saline, PBS (Sigma-Aldrich, USA) and stained

with 0.10% crystal violet solution for 10 min. Upon washing, 96% ethanol was added to each well and the results were read on a Biochrom EZ Read 400 microplate reader at 595 nm.

The experiment was performed in quadruplets and the results are given as mean value \pm STDEV. Descriptive statistical parameters were conducted using Microsoft Office 2013 Excel (Microsoft Corporation, Redmond, USA). The biofilm forming category was determined according to Stepanović *et al.* (2007), using the Biofilm Classifier Software version 1.1, where the optical density cut-off value (ODc) was calculated as three standard deviations above the mean OD of the negative control, while the biofilm categories were determined accordingly: $\text{OD} \leq \text{ODc}$: non-adherent, $\text{ODc} < \text{OD} \leq 2 \times \text{ODc}$: weakly adherent, $2 \times \text{ODc} < \text{OD} \leq 4 \times \text{ODc}$: moderately adherent, and $4 \times \text{ODc} < \text{OD}$: strongly adherent. The percentage of biofilm inhibition was calculated according to Jadhav *et al.* (2013).

RESULTS AND DISCUSSION

Two new Co(II) complexes Co(L1)_2 and Co(L2)_2 (where L1 is 2-((2-chlorobenzylidene) amino)-3-mercaptopropanoic acid and L2 is 3-mercapto-2-[(2-methoxybenzylidene) amino] propanoic acid), have been prepared by the reaction of metal salt ($\text{CoCl}_2 \cdot 6\text{H}_2\text{O}$) and Schiff base ligands. According to spectroscopic analyses, ligands (Schiff bases) coordinate to cobalt ion as the bidentate NO ligand.

The reaction scheme and the proposed structure of the Co(II) complexes are presented in Figure 1.

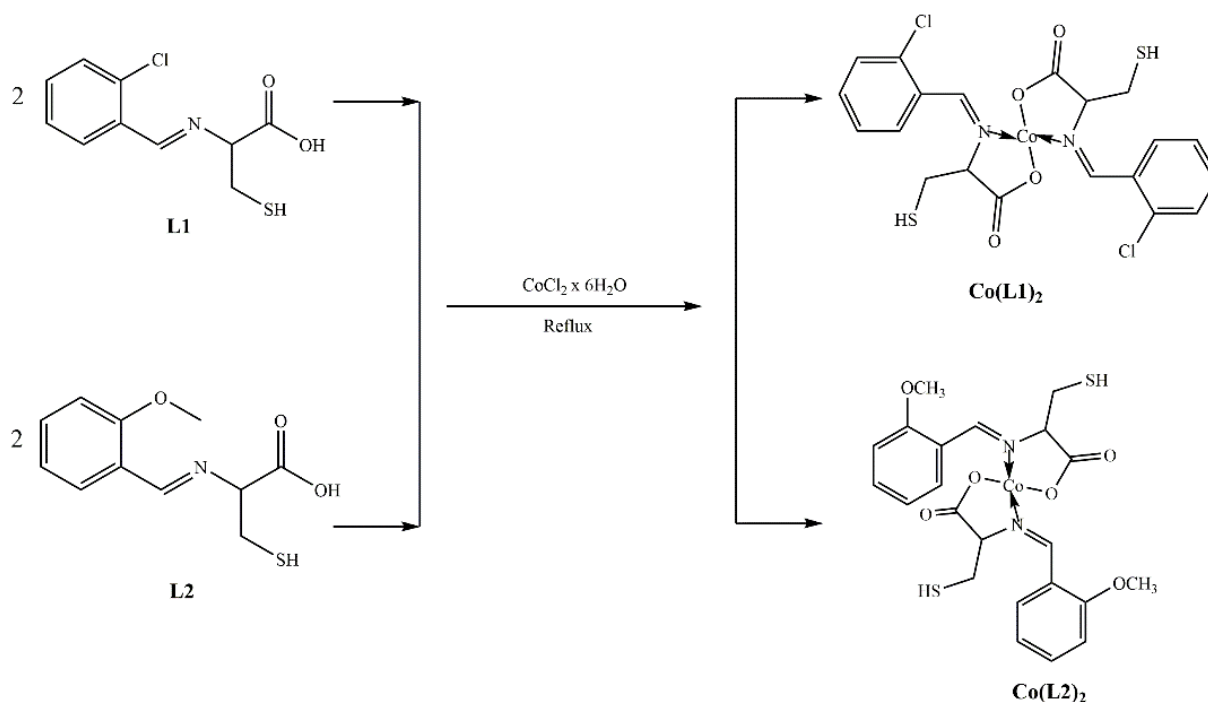


Figure 1: Reaction scheme and proposed structure of the Co(II) complexes.

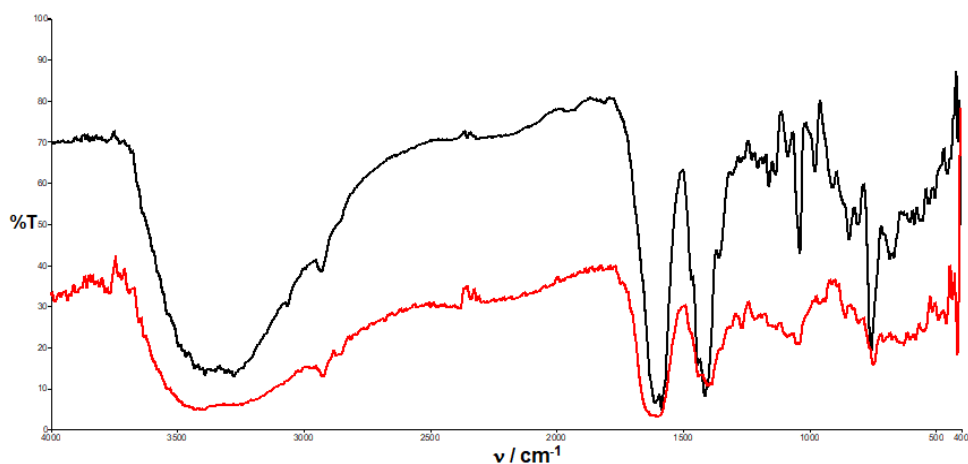


Figure 2: IR spectra of L1 (black spectra) and Co(L1)₂ (red spectra).

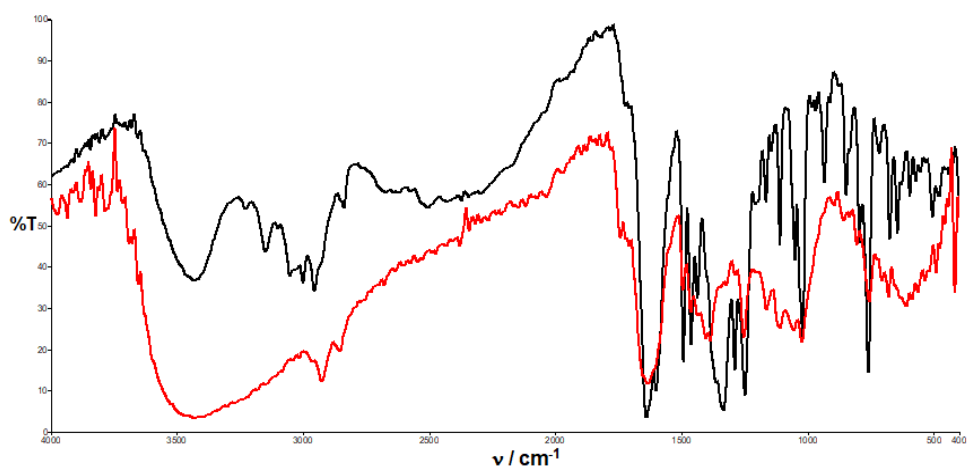


Figure 3: IR spectra of L2 (black spectra) and Co(L2)₂ (red spectra).

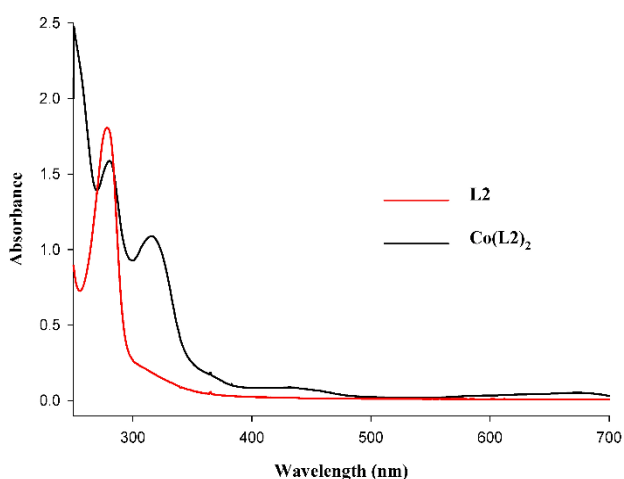


Figure 4: Representative UV spectra for L2 and Co(L2)₂.

Infrared spectra data

The IR spectra of the Schiff base (L1) derived from 2-chlorobenzaldehyde and *L*-cysteine and the synthesized complex Co(L1)₂ are given in Figure 2.

The IR spectra of the Schiff base (L2) derived from 2-methoxybenzaldehyde and *L*-cysteine and the synthesized complex Co(L2)₂ are given in Figure 3. Also, the UV-Vis spectra for L2 and Co(L2)₂ are shown in Figure 4.

The FTIR data confirm the coordination of the ligands *via* azomethine nitrogen and deprotonated carboxylate oxygen. In the FTIR spectra of the uncoordinated ligands L1 and L2, the bands observed at 1611 and 1639 cm⁻¹ correspond to the stretching frequencies of the azomethine group (Salihović *et al.*, 2021). In the Co(L1)₂ this band was observed at 1602 cm⁻¹, while in Co(L2)₂ at 1628 cm⁻¹. This shifts toward lower wave numbers indicating coordination of ligands to the Co(II) through

azomethine nitrogen (Salama *et al.*, 2017; Adiguzel *et al.*, 2018). The bands observed at 1357 (1336) cm^{-1} and 1442 (1467) cm^{-1} could be attributed to the symmetric and asymmetric stretching vibration of COO^- , respectively, in L1 (L2). In the spectra of the complexes, these bands are noticeable at 1400 and 1478 cm^{-1} in Co(L1)_2 and at 1385 and 1495 cm^{-1} in Co(L2)_2 . These frequencies were shifted towards higher wave numbers, which is indicative of the coordination of ligands to the Co(II) via deprotonated carboxylate oxygen (Selvaganapathy *et al.*, 2014). The bands appeared at 2928, and 2842 cm^{-1} in the spectra of Co(L1)_2 and Co(L2)_2 , respectively, assigned to the S-H stretching frequency remained unchanged, indicating that thiol sulphur is not involved in coordination. The new weak bands in Co(L1)_2 at 435 and 513 cm^{-1} could be assigned to the stretching vibration mode of Co-N and Co-O, respectively. These bands in Co(L2)_2 appear at 423 and 534 cm^{-1} (Al-Amery, 2014; Buldurun *et al.*, 2020). FTIR spectra of synthesized Co(II) complexes demonstrate that ligands act as bidentate O, N donor ligands.

Electronic spectra

To propose the geometrical structure of the newly synthesized Co(II) complexes, electronic absorption spectra of the Schiff bases and their complexes at the wavelength range from 250 to 700 nm were performed. The ligands (L1 and L2) showed absorption bands from 265 to 278.50 nm due to $\pi \rightarrow \pi^*$ transition of a benzene ring and other bands at 390 to 432 nm due to $n \rightarrow \pi^*$ transition of heteroatom C=N (Lu *et al.*, 2006). These bands were shifted to a higher or lower wavelength, which suggests nitrogen electron donation from Schiff bases to the Co(II) ion. Furthermore, the bands were identified in the 408-432 nm range, which could be attributed to charge transfer from ligand to metal. Another difference in the electronic spectra of the cobalt complex compared to the corresponding ligands is the appearance of very weak broad bands at 662.50 nm for Co(L1)_2 and 673 nm for Co(L2)_2 . These bands can be attributed to the $d-d$ transition of metal ions (Sakthivel *et al.*, 2021).

Determination of the MIC value

Obtained values of the minimum inhibitory concentration of Co(L1)_2 and Co(L2)_2 are summarized in Table 1.

The minimum inhibitory concentration for both tested substances was determined to be 250 $\mu\text{g/mL}$, except in the case of *E. coli* (Migula) Castellani and Chalmers ATCC 14169, where the MIC was determined to be 125 $\mu\text{g/mL}$ (Table 1). The previous investigation regarding the antimicrobial activity of Schiff's bases (Salihović *et al.*, 2021) showed that synthesized compounds possess antibacterial properties. This study confirmed the inhibitory potential of the novel Co(L1)_2 and Co(L2)_2 , with mostly balanced activity against Gram-positive and Gram-negative bacteria, including multidrug-resistant strains. In comparison to the antimicrobial activity of Schiff's bases [2-((2-chlorobenzylidene) amino)-3-mercaptopropanoic acid, and 3-mercapto-2-((2-methoxybenzylidene) amino) propanoic acid], their complexes performed higher antimicrobial activity, especially the Co(L2)_2 , where MIC of the Schiff base (ligand) for bacteria was 625 $\mu\text{g/mL}$ and MIC of its complex Co(L2)_2 was 125-250 $\mu\text{g/mL}$. The study of Saranya and Lakshmi (2015), investigated the antimicrobial activity of Co(II) complexes with similar structures, where the Schiff base used as the ligand was derived from *L*-cysteine and ketone. Their antibacterial capacity was higher in comparison to the Schiff base ligand and lower MIC values were detected, which is in accordance with our results. The results of Nair *et al.* (2012) also showed that the majority of the tested complexes were more active than their respective Schiff base ligand. This particular investigation involved the same binding mode as in our compounds, i.e., Schiff bases are coordinated to cobalt ions as bidentate ligands. According to Liang *et al.* (2021), cobalt complexes possess a broad spectrum of antimicrobial activity, including different cellular targets, where in some cases, their effects exceed the action of some common antibiotics. The potential explanation for the increased antibacterial activity of metal complexes compared to their ligands lies in their lipophilicity since that causes a higher entry rate into the lipid layer of the bacterial membranes.

Table 1: The minimum inhibitory concentration of Co(L1)_2 and Co(L2)_2 .

Bacterial strain	MIC ($\mu\text{g/mL}$)	
	Co(L1)_2	Co(L2)_2
<i>Staphylococcus aureus</i> subsp. <i>aureus</i> Rosenbach ATCC 6538	250	250
<i>S. aureus</i> subsp. <i>aureus</i> Rosenbach ATCC 25923	250	250
<i>S. aureus</i> subsp. <i>aureus</i> Rosenbach ATCC 33591	250	250
<i>S. aureus</i> NCTC 12493	250	250
<i>Enterococcus faecalis</i> ATCC 29212	250	250
<i>Bacillus subtilis</i> subsp. <i>spizizenii</i> ATCC 6633	250	250
<i>Escherichia coli</i> (Migula) Castellani and Chalmers ATCC 14169	125	125
<i>E. coli</i> (Migula) Castellani and Chalmers ATCC 25922	250	250
<i>E. coli</i> (Migula) Castellani and Chalmers ATCC 35218	250	250
<i>Salmonella enterica</i> subsp. <i>enterica</i> serotype Abony NCTC 6017	250	250
<i>Pseudomonas aeruginosa</i> ATCC 27853	250	250

Additionally, dipole moment and solubility may be potential reasons for the enhanced antibacterial activity of the complexes (Soltani *et al.*, 2020).

Our results suggest that analysed complexes don't possess bactericidal properties. There was no minimum bactericidal concentration since bacteria grew on agar plates upon exposure to all tested concentrations of the examined substances.

Evaluation of the antibiofilm activity

According to the positive control, all investigated Gram-positive bacteria performed capacity to form moderately adherent biofilm. In SA1, there was no change in the biofilm-forming category after exposure to Co(L1)₂, but biofilm inhibition was still recorded in all subinhibitory concentrations. Dilution of 125 µg/mL of Co(L1)₂ inhibited biofilm in the amount of 11.58% (Table 2). Co(L2)₂ caused moderate inhibition of the SA1 biofilm (0.50–35.36%) in the range of 125-15.63 µg/mL but with no change in the biofilm-forming category (Table 3). In SA2, Co(L1)₂ caused a decrease in the biofilm-forming capacity to weakly adherent in the range from 125 µg/mL (72.46%) to 15.63 µg/mL (58.45%) (Table 2), while Co(L2)₂ reduced the biofilm to weakly adherent only at the first subinhibitory concentration with inhibition of 50.87% (Table 3). SA3 biofilm was decreased to weakly adherent (inhibition of 33.11%) by the activity of Co(L1)₂ at 125 µg/mL (Table 2), while Co(L2)₂ caused biofilm inhibition in the amount of 14.33-41.87% and changed the biofilm-forming capacity in all subinhibitory concentrations (Table 3). SA4 biofilm-forming capacity was moderate in all subinhibitory concentrations of Co(L1)₂ (Table 2) and in the first three subinhibitory dilutions of Co(L2)₂ (Table 3). It could be seen that different *S. aureus* strains exhibit various responses to the tested compounds in terms of the biofilm-forming.

In general, biofilm formation in *S. aureus* is regulated through the accessory gene regulator (*agr*) quorum sensing system, and the most prominent compound is the so-called PIA (polysaccharide intercellular adhesin), the agent responsible for intercellular adhesion of the cells, and for the adhesion to external surfaces. This component is controlled by the intercellular adhesion (*ica*) locus, *icaADBC* and *icaR* (biosynthetic and regulatory) genes. The expression of *icaR* is related to the Staphylococcal accessory regulator A (SarA) and Sigma B (σ^B); while the Rbf protein (Regulator of biofilm formation) is the negative regulator of *icaR* gene, which is related to the enlarged *ica* gene expression, production of the PIA and biofilm formation. Biofilm inhibition is acquired by the regulation of *icaADBC* through the *spx* gene, a stress response effector of *icaR*. Many external factors could impact the *ica* locus (Parastan *et al.*, 2020). Chung *et al.* (2021) investigated the antibiofilm activity of copper-complexes derived from Schiff base and noted a significant reduction of biomass and metabolic activity in examined *S. aureus* strains, including MRSA.

In the case of *EF*, the biofilm-forming category was decreased to weakly adherent in the range of 31.25-1.95

µg/mL of Co(L1)₂ (Table 2), with the ascending inhibition percentage with lower concentrations (13.62-35.43%). Furthermore, Co(L2)₂ caused increasing in the biofilm-forming capacity of this strain in all subinhibitory concentrations (Table 3). *Enterococcus faecalis* is an opportunistic pathogen with increasing antibiotic resistance and an etiological agent of nosocomial infections (Kristich *et al.*, 2004). Due to the involvement of many virulent factors, understanding the biofilm formation of *E. faecalis* is still challenging. *BS* biofilm was inhibited by Co(L1)₂ in the range of 15.63-1.95 µg/mL (Table 2), in the amount of 17.49-36.13%, while Co(L2)₂ did not change the biofilm-forming category of this bacteria (Table 3). Co(L1)₂ decreased the biofilm-forming category of *EC1* to weakly adherent at concentrations of 62.50 and 32.25 µg/mL (Table 4), with inhibition of 65.50% and 55.84%, respectively and Co(L2)₂ exhibited inhibitory activity only at 62.50 µg/mL (Table 5), in the amount of 40.63%, but there was no change in the biofilm-forming category. *Bacillus subtilis* is soil bacteria and commensal species of the human gastrointestinal tract (Gingichashvili *et al.*, 2017). This bacteria combines two different life strategies, including biofilm formation and swimming motility, where the expression of the genes needed for biofilm formation (but not those for swimming motility) allowed this species to overcome unfavorable external conditions (Ryan-Payseur and Freitag, 2018). The expression of the matrix genes as the response to a particular external signal triggers the biofilm formation, but due to the numerous signals and mechanisms that could be related to the increased expression of extracellular matrix genes (Vlamakis *et al.*, 2013), additional studies are required for the identification of specific molecular mechanisms and signalization involved in the bacterial response in the mode of biofilm formation. *EC2* did not form a biofilm in all the replications of the positive control, while exposure to the tested compounds prompted bacteria to form a biofilm in subinhibitory concentrations (Tables 4 and 5). In the case of Co(L2)₂, strong biofilm was detected at 62.50-7.81 µg/mL (Table 5). *EC3* was evaluated as the strong biofilm former. Co(L1)₂ decreased the biofilm-forming category of this strain at 125-31.25 µg/mL (Table 4) with inhibition of 75.90-91.48% and Co(L2)₂ eliminated biofilm at 125 µg/mL (Table 5). Dilutions below 31.25 µg/mL of both Schiff base complexes did not have the capacity to change the biofilm-forming category of *EC3*. According to Sharma *et al.* (2016), many genes are involved in the biofilm formation of *E. coli*, such as those encoding different proteins located in the cell's inner membrane, peripheral membrane, cytoplasm, or represent multipass membrane proteins. Biofilm genes of *E. coli* that are frequently investigated are *csgD* (CsgBAC operon transcription regulatory protein regulates fimbriae production and positively affects biofilm formation and stress regulation), *hha* (haemolysin expression-modulating protein Hha repress the transcription of fimbrial genes and decrease biofilm formation), *bcsA* operon (cellulose synthase catalytic subunit catalyzes the cellulose formation), *pgaC* (poly-beta-1,6-N-acetyl-D-glucosamine synthase involved

Table 2: Mean absorbance values of Gram-positive bacteria biofilm formation in the presence of Co(L1)₂.

Tested concentration (µg/mL)	Tested bacteria											
	SA1		SA2		SA3		SA4		EF		BS	
	Value	CAT	Value	CAT	Value	CAT	Value	CAT	Value	CAT	Value	CAT
Negative control	0.062±0.002	NA	0.065±0.007	NA	0.059±0.002	NA	0.058±0.013	NA	0.064±0.002	NA	0.065±0.002	NA
Positive control	0.272±0.079	M	0.311±0.186	M	0.154±0.036	M	0.288±0.118	M	0.147±0.015	M	0.173±0.019	M
125	0.241±0.025	M	0.086±0.019	W	0.103±0.006	W	0.369±0.096	M	0.221±0.038	M	0.227±0.058	M
62.50	0.263±0.074	M	0.096±0.012	W	0.156±0.013	M	0.308±0.025	M	0.155±0.030	M	0.146±0.017	M
31.25	0.247±0.043	M	0.121±0.024	W	0.154±0.031	M	0.265±0.030	M	0.127±0.034	W	0.152±0.026	M
15.63	0.257±0.042	M	0.129±0.024	W	0.141±0.02	M	0.278±0.031	M	0.123±0.024	W	0.125±0.015	W
7.81	0.264±0.056	M	0.247±0.155	M	0.190±0.037	M	0.325±0.090	M	0.119±0.005	W	0.143±0.023	W
3.90	0.258±0.034	M	0.298±0.175	M	0.204±0.020	M	0.254±0.034	M	0.103±0.008	W	0.123±0.010	W
1.95	0.261±0.029	M	0.313±0.201	M	0.210±0.024	M	0.227±0.015	M	0.095±0.007	W	0.111±0.018	W

SA1: *Staphylococcus aureus* subsp. *aureus* Rosenbach ATCC 6538; SA2: *S. aureus* subsp. *aureus* Rosenbach ATCC 25923; SA3: *S. aureus* subsp. *aureus* Rosenbach ATCC 33591; SA4: *S. aureus* NCTC 12493; EF: *Enterococcus faecalis* ATCC 29212; BS: *Bacillus subtilis* subsp. *spizizenii* ATCC 6633. Values are mean ± STDEV. CAT: Biofilm category. Biofilm categories: NA - Non-adherent; W - Weakly adherent; M - Moderately adherent; S - Strongly adherent.

Table 3: Mean absorbance values of Gram-positive bacteria biofilm formation in the presence of Co(L2)₂.

Tested concentration (µg/mL)	Tested bacteria											
	SA1		SA2		SA3		SA4		EF		BS	
	Value	CAT	Value	CAT	Value	CAT	Value	CAT	Value	CAT	Value	CAT
Negative control	0.054±0.005	NA	0.065±0.002	NA	0.061±0.005	NA	0.052±0.005	NA	0.069±0.002	NA	0.066±0.008	NA
Positive control	0.250±0.032	M	0.201±0.072	M	0.155±0.035	M	0.227±0.030	M	0.210±0.019	M	0.199±0.042	M
125	0.162±0.017	M	0.099±0.013	W	0.091±0.023	W	0.241±0.010	M	0.308±0.072	S	0.268±0.032	M
62.50	0.179±0.014	M	0.211±0.139	M	0.091±0.024	W	0.195±0.009	M	0.375±0.075	S	0.246±0.009	M
31.25	0.228±0.009	M	0.259±0.076	M	0.090±0.021	W	0.203±0.031	M	0.378±0.021	S	0.225±0.036	M
15.63	0.249±0.022	M	0.229±0.070	M	0.097±0.025	W	0.338±0.083	S	0.302±0.047	S	0.206±0.030	M
7.81	0.297±0.027	S	0.257±0.199	M	0.099±0.036	W	0.315±0.072	S	0.305±0.011	S	0.206±0.014	M
3.90	0.318±0.121	S	0.159±0.049	M	0.133±0.043	W	0.382±0.040	S	0.317±0.075	S	0.220±0.042	M
1.95	0.286±0.068	S	0.148±0.055	M	0.126±0.030	W	0.358±0.122	S	0.318±0.066	S	0.315±0.144	M

SA1: *Staphylococcus aureus* subsp. *aureus* Rosenbach ATCC 6538; SA2: *S. aureus* subsp. *aureus* Rosenbach ATCC 25923; SA3: *S. aureus* subsp. *aureus* Rosenbach ATCC 33591; SA4: *S. aureus* NCTC 12493; EF: *Enterococcus faecalis* ATCC 29212; BS: *Bacillus subtilis* subsp. *spizizenii* ATCC 6633. Values are mean ± STDEV. CAT: Biofilm category. Biofilm categories: NA - Non adherent; W - Weakly adherent; M - Moderately adherent; S - Strongly adherent.

Table 4: Mean absorbance values of Gram-negative bacteria biofilm formation in the presence of Co(L1)₂.

Tested concentration (µg/mL)	Tested bacteria									
	EC1		EC2		EC3		SE		PA	
	Value	CAT	Value	CAT	Value	CAT	Value	CAT	Value	CAT
Negative control	0.066 ± 0.011	NA	0.069 ± 0.008	NA	0.061 ± 0.003	NA	0.060 ± 0.004	NA	0.065 ± 0.004	NA
Positive control	0.373 ± 0.120	M	0.068 ± 0.008	NA	1.054 ± 0.049	S	0.065 ± 0.006	NA	1.308 ± 0.310	S
125	0.073 ± 0.012	NA*	0.080 ± 0.012	NA	0.090 ± 0.020	W	0.059 ± 0.002	NA	0.311 ± 0.447	S
62.50	0.129 ± 0.013	W	0.067 ± 0.004	NA	0.254 ± 0.120	M	0.075 ± 0.006	W	0.891 ± 0.143	S
31.25	0.165 ± 0.033	W	0.072 ± 0.012	NA	0.208 ± 0.071	M	0.085 ± 0.005	W	1.299 ± 0.555	S
15.63	0.296 ± 0.058	M	0.082 ± 0.010	NA	0.768 ± 0.071	S	0.082 ± 0.003	W	1.195 ± 0.237	S
7.81	0.396 ± 0.131	M	0.121 ± 0.018	W	0.743 ± 0.174	S	0.080 ± 0.006	W	1.774 ± 0.491	S
3.90	0.362 ± 0.096	M	0.112 ± 0.010	W	0.649 ± 0.381	S	0.076 ± 0.004	W	1.336 ± 0.224	S
1.95	0.314 ± 0.069	M	0.171 ± 0.018	W	1.047 ± 0.157	S	0.075 ± 0.012	W	1.580 ± 0.633	S

EC1: *Escherichia coli* (Migula) Castellani and Chalmers ATCC 14169; EC2: *E. coli* (Migula) Castellani and Chalmers ATCC 25922; EC3: *E. coli* (Migula) Castellani and Chalmers ATCC 35218 (ESBL); SE: *Salmonella enterica* subsp. *enterica* serotype Abony NCTC 6017; PA: *Pseudomonas aeruginosa* ATCC 27853. Values are mean ± STDEV. CAT: Biofilm category. Biofilm categories: NA - Non adherent; W - Weakly adherent; M - Moderately adherent; S - Strongly adherent. *MIC for EC1 is at 125 µg/mL.

Table 5: Mean absorbance values of Gram-negative bacteria biofilm formation in the presence of Co(L2)₂.

Tested concentration (µg/mL)	Tested bacteria									
	EC1		EC2		EC3		SE		PA	
	Value	CAT	Value	CAT	Value	CAT	Value	CAT	Value	CAT
Negative control	0.058 ± 0.011	NA	0.060 ± 0.003	NA	0.052 ± 0.008	NA	0.059 ± 0.006	NA	0.059 ± 0.002	NA
Positive control	0.316 ± 0.034	M	0.064 ± 0.004	NA	0.445 ± 0.058	S	0.062 ± 0.005	NA	1.053 ± 0.161	S
125	0.074 ± 0.003	NA*	0.063 ± 0.001	NA	0.065 ± 0.005	NA	0.063 ± 0.007	NA	0.270 ± 0.055	S
62.50	0.188 ± 0.015	M	0.812 ± 0.055	S	0.122 ± 0.035	W	0.081 ± 0.016	W	0.422 ± 0.099	S
31.25	0.367 ± 0.034	S	1.014 ± 0.041	S	0.219 ± 0.039	M	0.127 ± 0.020	W	0.445 ± 0.106	S
15.63	0.413 ± 0.023	S	0.719 ± 0.038	S	0.321 ± 0.084	S	0.091 ± 0.012	W	0.789 ± 0.207	S
7.81	0.482 ± 0.022	S	0.386 ± 0.019	S	0.351 ± 0.098	S	0.080 ± 0.009	W	0.939 ± 0.108	S
3.90	0.540 ± 0.018	S	0.111 ± 0.020	W	0.383 ± 0.135	S	0.087 ± 0.030	W	1.020 ± 0.108	S
1.95	0.510 ± 0.046	S	0.079 ± 0.023	W	0.305 ± 0.121	S	0.077 ± 0.017	W	1.829 ± 0.414	S

EC1: *Escherichia coli* (Migula) Castellani and Chalmers ATCC 14169; EC2: *E. coli* (Migula) Castellani and Chalmers ATCC 25922; EC3: *E. coli* (Migula) Castellani and Chalmers ATCC 35218 (ESBL); SE: *Salmonella enterica* subsp. *enterica* serotype Abony NCTC 6017; PA: *Pseudomonas aeruginosa* ATCC 27853. Values are mean ± STDEV. CAT: Biofilm category. Biofilm categories: NA - Non adherent; W - Weakly adherent; M - Moderately adherent; S - Strongly adherent. *MIC for EC1 is at 125 µg/mL.

in the PGA polymer synthesis, which helps the adhesion of biofilm), *fimB* (regulatory protein-FimB regulates type 1 fimbriae production). *Salmonella enterica* subsp. *enterica* serotype Abony did not form biofilm in this experiment, but exposure to the investigated substances caused the formation of weakly adherent biofilm at lower concentrations (Tables 4 and 5). Biofilm formation in *Salmonella* species is mainly characterized by the EPS matrix consisting of proteins, carbohydrates, and extracellular DNA (eDNA). At the same time, exact composition may vary in dependence on environmental conditions, as well as the transition of planktonic *Salmonella* into the biofilm state is directed by temperature fluctuations, nutrient availability, exposure to harmful substances, etc. (Harrell *et al.*, 2021). Our investigation showed that analyzed complexes act as inhibitory agents for tested *Salmonella* strain, so we can speculate that the formation of the biofilm from the planktonic state, in this case, represents some sort of bacterial stress response. The control and integration of *Salmonella* biofilms are mainly regulated by the *csgD* factor, which is a transcriptional response regulator containing an N-terminal receiver domain with a conserved aspartate and a C-terminal LuxR-like helix-turn-helix (HTH) DNA-binding motif. In a genomic context, *csgD* is an integral part of the curli biosynthesis system (Steenackers *et al.*, 2012). *Pseudomonas aeruginosa* is evaluated as the strong biofilm former, and tested complexes did not change its biofilm-forming capacity (Tables 4 and 5). *Pseudomonas aeruginosa* is a life-threatening bacterial species whose pathogenicity and severity of infections are related to its excellent biofilm-forming capacity (Crespo *et al.*, 2018). Four separate quorum sensing pathways were described in the *P. aeruginosa*: Las, Rhl, PQS and IQS, with the Las system being at the top of the hierarchy. The first two quorum sensing circuits are triggered by the increased cell density at the preliminary exponential growth phase, while the other two are activated later in the exponential growth phase. Our investigation confirmed the strong biofilm-forming potential of *P. aeruginosa*. Overall results suggest that the investigated Schiff's base complexes possess antibiofilm activity in a manner that is strain-specific and concentration-dependent. According to the available literature and to the best of our knowledge, this study represents the first report regarding the antibiofilm activity of the Schiff base-derived cobalt(II) complexes.

CONCLUSION

New Co(II) Schiff base complexes were synthesized, spectrally characterized, and tested for antimicrobial activity. The synthesis was carried out using previously synthesized Schiff bases as ligands and cobalt(II) chloride hexahydrate. The FTIR spectral analysis showed characteristic shifts, which indicate that the Schiff bases act as bidentate ON ligands. Within the UV spectrum of the Schiff bases has been detected the existence of two absorption bands assigned to the transition $\pi \rightarrow \pi^*$ and $n \rightarrow \pi^*$. In the metal complex, these bands were shifted,

suggesting the transfer of electrons from ligands to the cobalt ion. This investigation showed that the novel complexes have inhibitory potential against different bacterial species, which is higher than the Schiff bases.

Furthermore, the performed study noted inhibitory potential against multidrug-resistant strains. Examined complexes also expressed antibiofilm activity. Considering the emergence of bacterial resistance to antimicrobial drugs and the impact of biofilm-associated infections on global health, describing novel antimicrobial agents is of great importance.

REFERENCES

- Abu-Dief, A. M. and Mohamed, I. M. (2015).** A review on versatile applications of transition metal complexes incorporating Schiff bases. *Beni-Suef University Journal of Basic and Applied Sciences* **4(2)**, 119-133.
- Abu-Yamin, A., Abduh, M. S., Saghir, S. A. M. and Al-Gabri, N. (2022).** Synthesis, characterization and biological activities of new Schiff base compound and its lanthanide complexes. *Pharmaceuticals* **15(4)**, 454.
- Adiguzel, R., Turan, N., Buldurun, K. and Korkoca, H. (2018).** Spectral, thermal and antimicrobial properties of novel mixed ligand-metal complexes derived from saccharinate complexes and azo dye ligand. *International Journal of Pharmacology* **14**, 9-19.
- Al-Amery, M. (2014).** Synthesis and characterization of new complexes of 2-(2-hydroxy phenyl)-2-N-amino (4-chloro-benzothiazol-2-yl) acetonitrile ligand with some divalent transition metal ions. *International Journal of Science and Research* **3(11)**, 3059-3064.
- Ambika, S., Manojkumar, Y., Arunachalam, S., Gowdhami, B., Sundaram, K. K. M., Solomon, R. V. et al. (2019).** Biomolecular interaction, anti-cancer and anti-angiogenic properties of cobalt(III) Schiff base complexes. *Scientific Reports* **9**, 2721.
- Bajema, E. A., Roberts, K. F. and Meade, T. J. (2019).** Cobalt-Schiff base complexes: Preclinical research and potential therapeutic uses. *In: Essential Metals in Medicine: Therapeutic Use and Toxicity of Metal Ions in the Clinic.* Carver, P. L. (eds.). De Gruyter, Berlin, Boston. pp. 267-302.
- Banerjee, A. and Chattopadhyay, S. (2019).** Synthesis and characterization of mixed valence cobalt(III)/cobalt(II) complexes with N, O-donor Schiff base ligands. *Polyhedron* **159**, 1-11.
- Buldurun, K., Turan, N., Bursal, E., Mantarci, A., Turkan, F., Taslimi, P. et al. (2020).** Synthesis, spectroscopic properties, crystal structures, antioxidant activities and enzyme inhibition determination of Co(II) and Fe(II) complexes of Schiff base. *Research on Chemical Intermediates* **46(1)**, 283-297.
- Chung, P. Y., Khoo, R. E. Y., Liew, H. S. and Low, M. L. (2021).** Antimicrobial and antibiofilm activities of Cu(II) Schiff base complexes against methicillin-susceptible and resistant *Staphylococcus aureus*. *Annals of Clinical Microbiology and Antimicrobials* **20**, 67.

- CLSI, Clinical and Laboratory Standards Institute. (2018).** Methods for Dilution Antimicrobial Susceptibility Test for Bacteria That Grow Aerobically, 11th ed. CLSI standard M07. Clinical and Laboratory Institute, Wayne, PA.
- Crespo, A., Blanco-Cabra, N. and Torrents, E. (2018).** Aerobic vitamin B₁₂ biosynthesis is essential for *Pseudomonas aeruginosa* class II ribonucleotide reductase activity during planktonic and biofilm growth. *Frontiers in Microbiology* **9**, 986.
- Gingichashvili, S., Duanis-Assaf, D., Shemesh, M., Featherstone, J. D. B., Feuerstein, O. and Steinberg, D. (2017).** *Bacillus subtilis* biofilm development – A computerized study of morphology and kinetics. *Frontiers in Microbiology* **8**, 2072.
- Gupta, K. C. and Sutar, A. K. (2008).** Catalytic activities of Schiff base transition metal complexes. *Coordination Chemistry Reviews* **252(12-14)**, 1420-1450.
- Harrell, J. E., Hahn, M. M., D'Souza, S. J., Vasicek, E. M., Sandala, J. L., Gunn, J. S. et al. (2021).** *Salmonella* biofilm formation, chronic infection, and immunity within the intestine and hepatobiliary tract. *Frontiers in Cellular and Infection Microbiology* **10**, 624622.
- Hossain, M. S., Roy, P. K., Zakaria, C. M. and Kudrat-E-Zahan, M. (2018).** Selected Schiff base coordination complexes and their microbial application: A review. *International Journal of Chemical Studies* **6(1)**, 19-31.
- Jadhav, S., Shah, R., Bhave, M. and Palombo, E. A. (2013).** Inhibitory activity of yarrow essential oil on *Listeria* planktonic cells and biofilms. *Food Control* **29(1)**, 125-130.
- Kar, K., Ghosh, D., Kabi, B. and Chandra, A. (2022).** A concise review on cobalt Schiff base complexes as anticancer agents. *Polyhedron* **222**, 115890.
- Kristich, C. J., Li, Y. H., Cvitkovitch, D. G. and Dunny, G. M. (2004).** Esp-independent biofilm formation by *Enterococcus faecalis*. *Journal of Bacteriology* **186(1)**, 154-163.
- Liang, J., Sun, D., Yang, Y., Li, M., Li, H. and Chen, L. (2021).** Discovery of metal-based complexes as promising antimicrobial agents. *European Journal of Medicinal Chemistry* **224**, 113696.
- Lu, Y. H., Lu, Y. W., Wu, C. L., Shao, Q., Chen, X. L. and Bimbong, R. N. B. (2006).** UV-visible spectroscopic study of the salicylaldehyde benzoylhydrazone and its cobalt complexes. *Spectrochimica Acta Part A: Molecular and Biomolecular Spectroscopy* **65(3-4)**, 695-701.
- Merritt, J. H., Kadouri, D. E. and O'Toole, G. A. (2005).** Growing and analyzing static biofilms. *Current Protocols in Microbiology* **Chapter 1, Unit-1B.1**.
- Nair, M. S., Arish, D. and Joseyphus, R. S. (2012).** Synthesis, characterization, antifungal, antibacterial and DNA cleavage studies of some heterocyclic Schiff base metal complexes. *Journal of Saudi Chemical Society* **16(1)**, 83-88.
- Nejo, A. A., Kolawole, G. A. and Nejo, A. O. (2010).** Synthesis, characterization, antibacterial, and thermal studies of unsymmetrical Schiff-base complexes of cobalt(II). *Journal of Coordination Chemistry* **63(24)**, 4398-4410.
- Parastan, R., Kargar, M., Solhjoo, K. and Kafilzadeh, F. (2020).** *Staphylococcus aureus* biofilms: Structures, antibiotic resistance, inhibition, and vaccines. *Gene Reports* **20**, 100739.
- Rajee, A. O., Babamale, H. F., Lawal, A., Aliyu, A. A., Osunniran, W. A., Sheriff, A. O. et al. (2021).** Mn(II), Co(II), Ni(II), and Cu(II) complexes of amino acid derived Schiff base ligand: Synthesis, characterization and *in-vitro* antibacterial investigations. *Bulletin of the Chemical Society of Ethiopia* **35(1)**, 97-106.
- Ryan-Payseur, B. K. and Freitag, N. E. (2018).** *Bacillus subtilis* biofilms: A matter of individual choice. *mBio* **9(6)**, e02339-18.
- Sakthivel, R. V., Sankudevan, P., Vennila, P., Venkatesh, G., Kaya, S. and Serdaroglu, G. (2021).** Experimental and theoretical analysis of molecular structure, vibrational spectra and biological properties of the new Co(II), Ni(II) and Cu(II) Schiff base metal complexes. *Journal of Molecular Structure* **1233**, 130097.
- Salama, M. M., Ahmed, S. G. and Hassan, S. S. (2017).** Synthesis, characterizations, biological, and molecular docking studies of some amino acid Schiff bases with their cobalt (II) complexes. *Advances in Biological Chemistry* **7(5)**, 182-194.
- Salihović, M., Pazalja, M., Mahmutović-Dizdarević, I., Jerković-Mujkić, A., Suljagić, J., Špirtović-Halilović, S. et al. (2018).** Synthesis, DFT study and antimicrobial activity of Schiff bases derived from benzaldehydes and amino acids. *Rasayan Journal of Chemistry* **11(3)**, 1074-1083.
- Salihović, M., Pazalja, M., Špirtović-Halilović, S., Veljović, E., Mahmutović-Dizdarević, I., Roca, S. et al. (2021).** Synthesis, characterization, antimicrobial activity, and DFT study of some novel Schiff bases. *Journal of Molecular Structure* **1241**, 130670.
- Saranya, J. and Lakshmi, S. S. (2015).** *In vitro* antioxidant, antimicrobial and larvicidal studies of Schiff base transition metal complexes. *Journal of Chemical and Pharmaceutical Research* **7**, 180-186.
- Selvaganapathy, M., Pravin, N., Pothiraj, K. and Raman, N. (2014).** Photo biological activation of NSO donor mixed-ligand complexes: *In vivo* and preclinical perspectives. *Journal of Photochemistry and Photobiology B: Biology* **138**, 256-272.
- Shah, S. S., Shah, D., Khan, I., Ahmad, S., Ali, U. and Rahman, A. (2020).** Synthesis and antioxidant activities of Schiff bases and their complexes: An updated review. *Biointerface Research in Applied Chemistry* **10(6)**, 6936-6963.
- Sharma, G., Sharma, S., Sharma, P., Chandola, D., Dang, S., Gupta, S. et al. (2016).** *Escherichia coli* biofilm: Development and therapeutic strategies. *Journal of Applied Microbiology* **121(2)**, 309-319.

- Siraj, I. T. and Sanusi, S. (2021).** Synthesis, characterization and antimicrobial studies of Co(II) and Ni(II) Schiff base complexes derived from furfuraldehyde and sulfamethoxazole. *International Journal of Scientific Research in Chemistry* **6(4)**, 01-09.
- Skrodzki, M., Patroniak, V. and Pawluć, P. (2021).** Schiff base cobalt(II) complex-catalyzed highly Markovnikov-selective hydrosilylation of alkynes. *Organic Letters* **23(3)**, 663-667.
- Soltani, B., Ghorbanpour, M., Ziegler, C. J., Ebadi-Nahari, M. and Mohammad-Rezaei, R. (2020).** Nickel (II) and cobalt (II) complexes with bidentate nitrogen-sulfur donor pyrazole derivative ligands: Synthesis, characterization, X-ray structure, electrochemical studies, and antibacterial activity. *Polyhedron* **180**, 114423.
- Steenackers, H., Hermans, K., Vanderleyden, J. and De Keersmaecker, S. C. J. (2012).** *Salmonella* biofilms: An overview on occurrence, structure, regulation and eradication. *Food Research International* **45(2)**, 502-531.
- Stepanović, S., Vuković, D., Hola, V., Di Bonaventura, G., Djukić, S., Cirković, I. et al. (2007).** Quantification of biofilm in microtiter plates: Overview of testing conditions and practical recommendations for assessment of biofilm production by staphylococci. *APMIS* **115(8)**, 891-899.
- Tsantis, S. T., Tzimopoulos, D. I., Holynska, M. and Perlepes, S. P. (2020).** Oligonuclear actinoid complexes with Schiff bases as ligands—Older achievements and recent progress. *International Journal of Molecular Sciences* **21(2)**, 555.
- Vlamakis, H., Chai, Y., Beauregard, P., Losick, R. and Kolter, R. (2013).** Sticking together: Building a biofilm the *Bacillus subtilis* way. *Nature Reviews Microbiology* **11(3)**, 157-168.